Radiochemistry and Preclinical PET Imaging of 68Ga-Desferrioxamine Radiotracers Targeting Prostate-Specific Membrane Antigen

Gourni, Eleni ; et al ; Holland, Jason P

Abstract: Radiotracers incorporating the urea-based Glu-NH-C(O)-NH-Lys group have gained prominence due to their role in targeting prostate-specific membrane antigen (PSMA)—a clinical biomarker of prostate cancer. Here, the synthesis, radiolabeling, and in vitro and in vivo characterization of two 68Ga-radiolabeled Glu-NH-C(O)-NH-Lys radiotracers conjugated to the desferrioxamine B (DFO) chelate were evaluated. Two linker groups based on amide bond and thiourea coupling chemistries were employed to develop 68Ga-DFO-Nsucc-PSMA (68Ga-4) and 68Ga-DFO-pNCS-Bn-PSMA (68Ga-7), respectively. Radiosynthesis proceeded quantitatively at room temperature with high radiochemical yields, chemical/radiochemical purities, and specific activities. Pharmacokinetic profiles of 68Ga-4 and 68Ga-7 were assessed using positron-emission tomography (PET) in mice bearing subcutaneous LNCaP tumors. Data were compared to the current clinical benchmark radiotracer 68Ga-HBED-CC-PSMA (68Ga-1) (HBED ¼ N,N0-Bis(2-hydroxy-5-(ethylene-beta-carboxy)benzyl)ethylenediamine N,N0-diacetic acid). Results indicated that the target binding affinity, protein association, blood pool and background organ clearance properties, and uptake in PSMApositive lesions are strongly dependent on the nature of the chelate, the linker, and the spacer groups. Protein dissociation constants (Kd values) were found to be predictive of pharmacokinetics in vivo. Compared to 68Ga-1, 68Ga-4 and 68Ga-7 resulted in decreased tumor uptake but enhanced blood pool clearance and reduced residence time in the kidney. The study highlights the importance of maximizing protein binding affinity during radiotracer optimization.

DOI: https://doi.org/10.1177/1536012117737010

Article

Radiochemistry and Preclinical PET Imaging of ^{68}Ga-Desferrioxamine Radiotracers Targeting Prostate-Specific Membrane Antigen

Molecular Imaging
Volume 16: 1-11

DOI: 10.1177/1536012117737010
journals.sagepub.com/home/mix
SAGE

Eleni Gourni, PhD[1,2,3], Luigi Del Pozzo, BSc[1,2,3], Mark Bartholomä, PhD[2], Yvonne Kiefer, BSc[2], Philipp T. Meyer, MD, PhD[1,2], Helmut R. Maecke, PhD[2], and Jason P. Holland, D.Phil[1,2,3,4]

Abstract

Radiotracers incorporating the urea-based Glu-NH-C(O)-NH-Lys group have gained prominence due to their role in targeting prostate-specific membrane antigen (PSMA)—a clinical biomarker of prostate cancer. Here, the synthesis, radiolabeling, and in vitro and in vivo characterization of two ^{68}Ga-radiolabeled Glu-NH-C(O)-NH-Lys radiotracers conjugated to the desferrioxamine B (DFO) chelate were evaluated. Two linker groups based on amide bond and thiourea coupling chemistries were employed to develop ^{68}Ga-DFO-Nsucc-PSMA (^{68}Ga-4) and ^{68}Ga-DFO-*p*NCS-Bn-PSMA (^{68}Ga-7), respectively. Radiosynthesis proceeded quantitatively at room temperature with high radiochemical yields, chemical/radiochemical purities, and specific activities. Pharmacokinetic profiles of ^{68}Ga-4 and ^{68}Ga-7 were assessed using positron-emission tomography (PET) in mice bearing subcutaneous LNCaP tumors. Data were compared to the current clinical benchmark radiotracer ^{68}Ga-HBED-CC-PSMA (^{68}Ga-1) (HBED = N,N′-Bis(2-hydroxy-5-(ethylene-beta-carboxy)benzyl)ethylenediamine N,N′-diacetic acid). Results indicated that the target binding affinity, protein association, blood pool and background organ clearance properties, and uptake in PSMA-positive lesions are strongly dependent on the nature of the chelate, the linker, and the spacer groups. Protein dissociation constants (K_d values) were found to be predictive of pharmacokinetics in vivo. Compared to ^{68}Ga-1, ^{68}Ga-4 and ^{68}Ga-7 resulted in decreased tumor uptake but enhanced blood pool clearance and reduced residence time in the kidney. The study highlights the importance of maximizing protein binding affinity during radiotracer optimization.

Keywords

gallium-68, prostate-specific membrane antigen (PSMA), positron-emission tomography, chelates, desferrioxamine

Introduction

Prostate-specific membrane antigen (PSMA; also known as glutamate carboxypeptidase II [GCPII] or *N*-acetyl-L-aspartyl-L-glutamate peptidase I [NAALADase I]) is an important class II membrane-bound zinc metalloenzyme that catalyzes the hydrolysis of *N*-acetylaspartylglutamate (NAAG) to glutamate and *N*-acetylaspatate (NAA).[1] The PSMA has emerged as a valuable preclinical and clinical biomarker of prostate cancer (PCa). Many prostate cancers, as well as other cancers that exhibit neoangiogenesis, express high levels of PSMA. Lower levels are found in physiologically normal tissues such as the kidneys, salivary glands, and small intestine.[2] Consequently, differential PSMA expression in PCa has led physicians and radiochemists to explore the use of PSMA as a target for delivering a wide range of diagnostic and radiotherapeutic nuclides.[3-5]

Worldwide, at least 50 clinical trials have investigated PSMA-targeted imaging or therapy in different populations of patients with PCa (source: www.clinicaltrials.gov). The two most important classes of drugs targeting PSMA are small-molecule urea-based inhibitors[4,6-12] and anti-PSMA

[1] German Cancer Consortium (DKTK), Heidelberg, Germany
[2] Faculty of Medicine, Department of Nuclear Medicine, Medical Center—University of Freiburg, University of Freiburg, Freiburg, Germany
[3] German Cancer Research Center (DKFZ), Heidelberg, Germany
[4] Department of Chemistry, University of Zurich, Zurich, Switzerland

Submitted: 30/06/2017. Revised: 03/08/2017. Accepted: 02/09/2017.

Corresponding Author:
Jason P. Holland, Department of Chemistry, University of Zurich, Winterthurerstrasse 190, CH-8057 Zurich, Switzerland.
Email: jason.holland@chem.uzh.ch

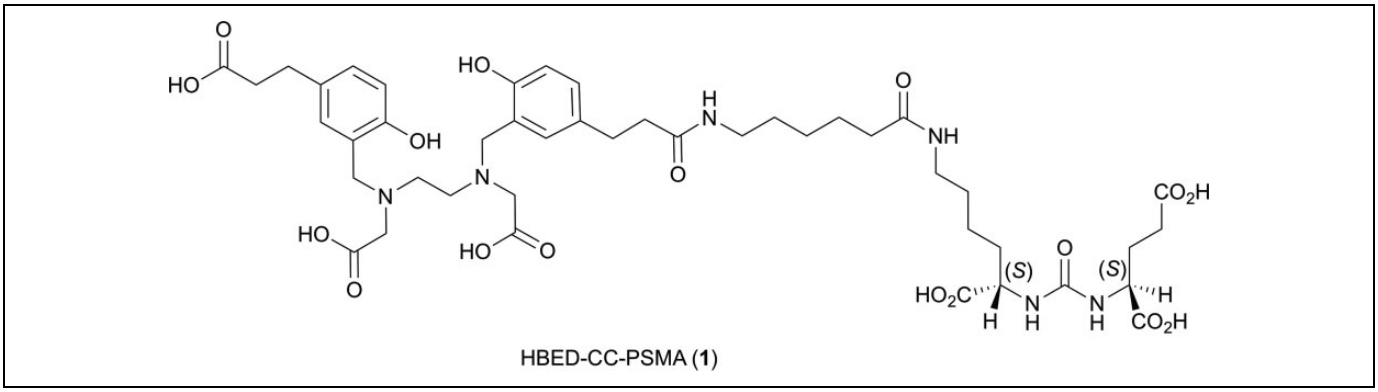

Figure 1. Structure of the HBED-CC- prostate-specific membrane antigen (PSMA) ligand (compound 1).

antibodies.[13-18] In terms of molecular imaging with positron-emission tomography (PET), the urea-based ^{68}Ga-HBED-CC-PSMA[19-24] (^{68}Ga-1; Figure 1) and antibody-based ^{89}Zr-DFO-J591[15-18] have shown promise for characterizing PSMA profiles in humans. For small-molecule PSMA inhibitors, the excellent clinical performance of ^{68}Ga-labeled agents for PET also prompted multicenter studies which demonstrated that ^{177}Lu-labeled analogues can be used to advance a novel "theranostic" (combined diagnostic imaging and radiotherapy) regimen.[25,26]

The synthesis and biological evaluation of a large number of Glu-NH-C(O)-NH-Lys inhibitors of PSMA have been reported.[6,27] Many radiolabeled analogues are also studied in vivo. Selected examples include work using the radionuclides fluorine-18,[28-31] copper-64,[11,32] gallium-68,[19,20,23,33] technetium .99m,[7,9,34] and various radiohalogens.[4,6,35] While recent studies have demonstrated that the performance of at least two ^{18}F-radiolabeled agents,^{18}F-DCFPyL[23] and ^{18}F-PSMA-6,[24] and the more recent compound ^{18}F-PSMA-1007,[36] compare favorably to that of ^{68}Ga-1; this ^{68}Ga-radiotracer remains the most well-characterized radiometal-based agent for PET imaging of PSMA. The radiosynthesis of ^{68}Ga-1 is well established—essentially quantitative radiolabeling can be achieved upon reacting the precursor HBED-CC-PSMA (compound 1) with ^{68}Ga in sodium acetate buffer at pH 4.5 for 10 minutes at 95°C.[19,20] Interestingly, the use of the HBED chelate has been suggested to lead to the potential formation of two diastereomers as resolved by high-performance liquid chromatography (HPLC).[20] The composition ratio of these two species depends on the pH and reaction temperature—data confirming that one isomer is thermodynamically more stable in aqueous solution and that intramolecular hydrogen bonding is likely to influence complex stability. Experimental studies in cells also showed that the two species have identical binding properties toward PSMA.[20] However, the formation of two isomers (in a variable ratio[20]) is unsatisfactory from the perspective of quality control (QC) in a clinical setting.

In this work, we synthesized and evaluated two new ^{68}Ga-labeled PSMA inhibitors bearing the *tris*-hydroxamic acid chelate desferrioxamine B (DFO). Two bifunctional versions of DFO (DFO-Nsucc [2] and DFO-*p*NCS-Bn [5]; Figure 2) with varying lipophilic character of the linker/spacer group were conjugated to Glu-NH-C(O)-NH-Lys-Ahx starting materials (compounds 3 and 6) to generate the radiolabeling precursors 4 and 7, respectively (Figure 2). Saturation binding assays in LNCaP cells, ex vivo protein binding and stability measurements, and PET imaging were used to compare the two new radiotracers ^{68}Ga-DFO-Nsucc-PSMA (^{68}Ga-4) and ^{68}Ga-DFO-*p*NCS-Bn-PSMA (^{68}Ga-7), to the clinical radiotracer ^{68}Ga-1. Results found that targeting of PSMA using urea-based radiometal complexes is highly sensitive to the chemical nature of the chelate and linker/spacer groups.

Materials and Methods

Standard laboratory techniques were employed throughout. Unless otherwise stated, all solvents and reagents were used as received from the supplier (SigmaAldrich [Darmstadt, Germany], TCI Deutschland [Eschborn, Germany], Acros [Geel, Belgium]). The HBED-CC-PSMA (also known as DKFZ-11) was purchased from ABX (Radeberg, Germany). Low-resolution electrospray ionization mass spectrometry ((+)-LR-ESI-MS) was performed on a PerkinElmer Flexar SQ 300 MS Detector (Waltham, MA). High-resolution electrospray ionization mass spectra ((+)-HR-ESI-MS) were measured by the Mass Spectrometry Service at the University of Zurich. HPLC was conducted on an Agilent 1260 Infinity System equipped with an Agilent 1200 DAD UV detector (UV detection at 220 nm) (Santa Clara, CA) equipped with Raytest radiation detector (Raytest GmbH, Straubenhardt, Germany) and a Chromolith Performance RP-18e 100-4.6 mm column (Merck, Billerica, MA). Typically, a water/acetonitrile gradient elution method (1.0 mL/min; 5 minutes; 5%-60% MeCN; UV detection at 220 nm and 320 nm) was used for analytical measurements (Chromolith method). Samples were lyophilized using a Christ Alpha 1-2 LD plus lyophilizer. All instruments measuring radioactivity were calibrated and maintained in accordance with previously reported routine QC procedures.[37] Radioactivity measurements were made using a calibrated Activimeter ISOMED 2010 (Nuklear-Medizintechnik, Dresden, Germany). For accurate quantification of radioactivity, experimental samples were counted for between 30 seconds

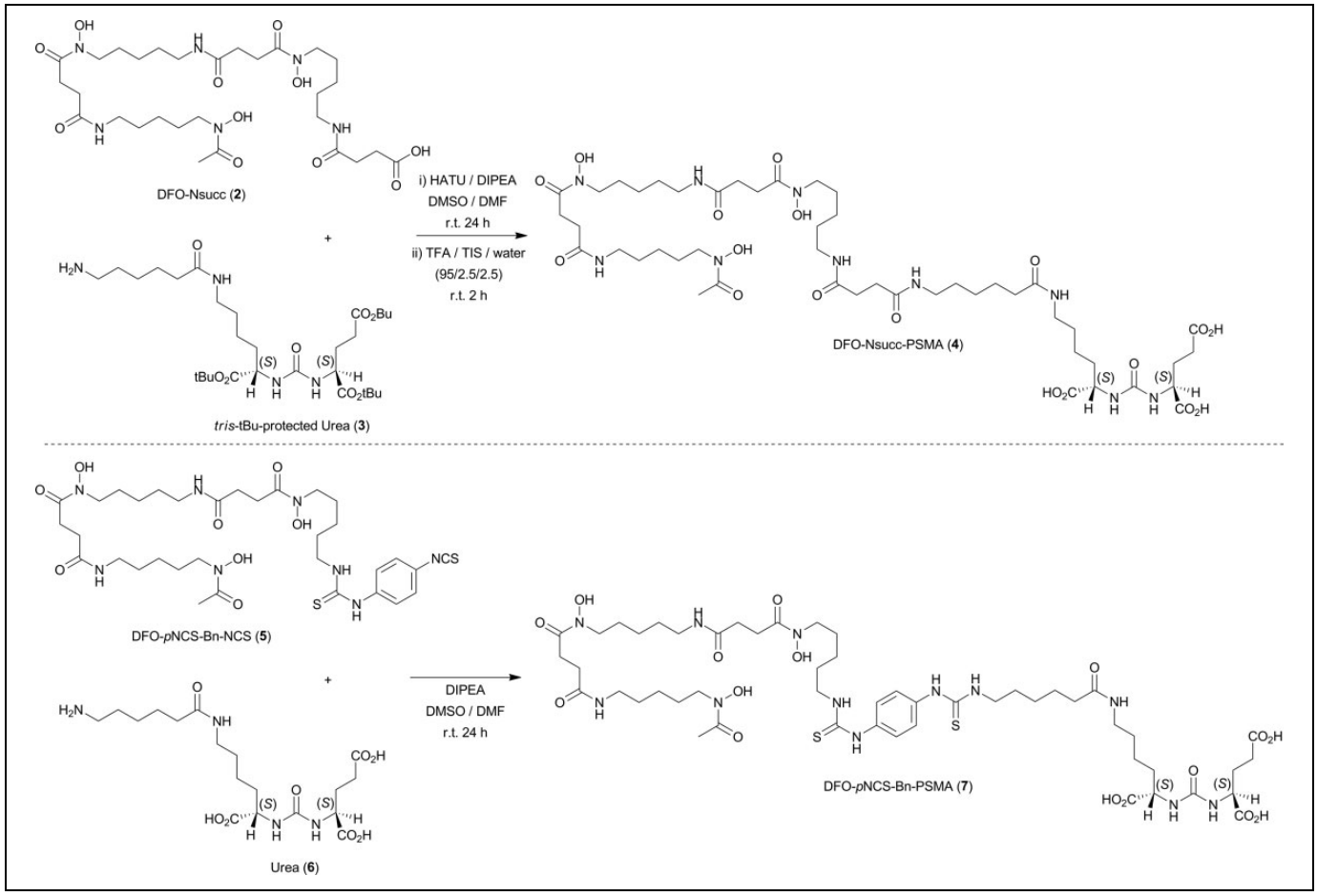

Figure 2. Coupling reactions used in the synthesis of desferrioxamine B (DFO)-Nsucc-prostate-specific membrane antigen (PSMA; compound 4) and DFO-*p*NCS-Bn-PSMA (compound 7).

and 1 minute on a calibrated PerkinElmer 2480 Automatic Wizard^2 Gamma Counter (Perkin Elmer, Waltham, Massachusetts). A dynamic energy window of 400 to 600 keV was used for ^{68} Ga (511 keV emission) detection.

Synthesis

The DFO-Nsucc-PSMA (4). The DFO was reacted with succinic anhydride in accordance with previously reported methods to give the reagent DFO-Nsucc (2).[38] The *tris*-tBu-protected urea (3) was purchased from ABX and used as received. The *tris*-tBu-protected urea (3; 5.2 mg, molecular weight [MW] 600.8 g/mol, 9.07 μmol) was dissolved in DMF (200 μL). DFO-Nsucc (2; 6.60 mg, MW 661.7 g/mol, 10.0 μmol) is only sparingly soluble in DMF and was dissolved in dimethyl sulfoxide (DMSO; 200 μL). 1-[Bis(dimethylamino)methylene]-1H-1,2,3-triazolo[4,5-b]pyridinium-3-oxide hexafluorophosphate (HATU; 4.0 mg, 1.16 equivalent) was dissolved in DMF (200 μL) to which *N*, *N*-diisopropylethylamine (DIPEA; 3.3 μL, 1.9 μmol, 2.1 equivalent) was added. The HATU/DIPEA mixture was added to the solution of compound 2 and then the resulting mixture was added to the solution of compound 3. The reaction was stirred at room temperature for 24 hours and progress was monitored by (+)-LR-ESI-MS. Then the DMF was evaporated and the crude product was deprotected by reaction with a trifluoroacetic acid/triisopropylsilane/water (TFA/TIS/H_2O; 95/2.5/2.5 v/v ratio) mixture (100 μL) for 2 hours at room temperature. The crude product was then precipitated by slow addition of diethyl ether, separated from the supernatant by centrifugation, and dissolved in 30% MeCN/H_2O. The crude product was purified by preparative HPLC on a Macherey-Nagel Nucleosil reverse phase C18 column (Oensingen, Germany) with a 10% to 45% MeCN/H_2O (0.1% TFA v/v added to both solvents) gradient over 12 minutes. On this HPLC system, the product eluted with a retention time (R_t) of 6.6 minutes. The product was lyophilized to give compound 4 as a white amorphous powder (1.6 mg, 1.5 μmol, 16%). The (+)-LR-ESI-MS *m/z* (30% MeCN/H_2O) 1076 (50%; $[M+H]^+ = C_{47}H_{84}N_{10}O_{18}{}^{2+}$) and 539 (100%; $[M+2\ H]^{2+} = C_{47}H_{84}N_{10}O_{18}{}^{2+}$). The (+)-HR-ESI-MS *m/z* (30% MeCN/H_2O) found 538.2981 (100%; $[M+2\ H]^{2+}$) calculated for $C_{47}H_{84}N_{10}O_{18}{}^{2+} = 538.2977$.

Test labeling reactions conducted in water at room temperature using compound 4 and nonradioactive $^{nat}Ga(NO3)_3$ gave the desired product ^{nat}Ga-DFO-Nsucc-PSMA (^{nat}Ga-4) in solution, with a single peak in reverse-phase (RP) HPLC (10%-45% MeCN/H_2O gradient. $R_t = 10.2$ minutes; >98%), (+)-LR-ESI-

MS *m/z* (30% MeCN/H_2O) 571 (100%; $[M+2H]^{2+}$), (+)-HR-ESI-MS *m/z* (30% MeCN/H_2O) found 571.2491 (100%; $[M+2H]^{2+}$), calculated for $C_{47}H_{81}N_{10}O_{18}Ga^{2+} = 571.2488$. Additional test reactions labeling compound 4 with $^{nat}FeCl_3$ gave an instantaneous and intense color change from colorless to a deep brown/orange solution, indicating the formation of an Fe-DFO complex of orange/brown with a known broad electronic absorption maximum at 430 nm ($\varepsilon_{430} = 2216 \pm 49$ mol/dm^3/cm).[16]

*The DFO-pNCS-Bn-PSMA (**7**).* Urea (6) was isolated by preparative HPLC after TFA/TIS/H_2O deprotection of *tris*-tBu-protected urea (3).[19] Urea (6; 1.2 mg, MW 432.5 g mol^{-1}, 2.8 μmol) was dissolved in DMF (250 μL). Separately, DFO-*p*NCS-Bn (5; Macrocyclics, Dallas, Texas; 2.3 mg, MW 752.8 g/mol, 3.1 μmol, 1.1 equivalent) was dissolved in DMSO (150 μL), and DIPEA (1.1 μL, 0.8 μmol, 2.2 equivalent) was added. Then the solution of compound 5 was added to the solution of compound 6, and the reaction was stirred for 24 hours at room temperature. Reaction progress was monitored by (+)-LR-ESI-MS. The crude reaction was then diluted with 2.1 mL H_2O, and the product was purified by preparative HPLC on a Macherey-Nagel Nucleosil reverse phase C18 column with a 10% to 45% MeCN/H_2O (0.1% TFA v/v added to both solvents) gradient over 25 minutes. On this HPLC system, the product eluted with a retention time R_t of 13.0 to 13.8 min. The product was lyophilized to give compound 7 as a white amorphous powder (2.5 mg, 2.1 μmol, 76%). (+)-LR-ESI-MS *m/z* (50% MeCN/H_2O) 1186 (30%; $[M+H]^+ = C_{51}H_{85}N_{12}O_{16}S_2^+$) and 594 (100%; $[M+2H]^{2+} = C_{51}H_{86}N_{12}O_{16}S_2^{2+}$), (+)-HR-ESI-MS *m/z* (50% MeCN/H_2O) found 593.2877 (100%; $[M+2H]^{2+}$) calculated for $C_{51}H_{86}N_{12}O_{16}S_2^{2+}$ 593.2863.

Test labeling reactions conducted in water at room temperature using compound 7 and $^{nat}Ga(NO3)_3$ gave the desired product ^{nat}Ga-DFO-*p*NCS-Bn-PSMA (^{nat}Ga-7) in solution with a single peak in RP-HPLC (10-45% MeCN/H_2O gradient, R_t = 10.2 min; >98%), (+)-LR-ESI-MS *m/z* (30% MeCN/H_2O) 626 (100%; $[M+2H]^{2+} = C_{51}H_{83}GaN_{12}O_{16}S_2^{2+}$).

Radiochemistry

^{68}Ga-radiolabeling experiments were conducted either manually or using the Modular-Lab PharmTracer automated synthesis module (Eckert&Ziegler, Berlin, Germany). Briefly, the ^{68}Ge/^{68}Ga-generator (Eckert&Ziegler, Model IGG100 Gallium-68 Generator) was eluted with HCl (0.1 M, 7 mL) in accordance with the manufacturer's protocol. The eluate (~600 MBq) was loaded onto a cation exchange column (Strata-XC [SCX]; Phenomenex, Torrance, California), and ^{68}Ga was eluted from the SCX cartridge with 800 μL of a mixture of 0.13 mol/L HCl in ~5 mol/L NaCl(aq). For all automated syntheses, the ^{68}Ga eluate was transferred into the reaction vial containing the appropriate buffer and radiolabeling precursor (vide infra).

*Radiosynthesis of ^{68}Ga-HBED-CC-PSMA (^{68}Ga-**1**).* ^{68}Ga-HBED-PSMA (^{68}Ga-1)[19] was prepared in 10 minutes at 95°C, using the Modular-Lab PharmTracer module by Eckert & Ziegler (Berlin, Germany). The ^{68}Ga eluate (~600 MBq) was transferred into a preheated reaction vial containing sodium acetate (2 mL, ~1 mol/L, pH4.5), HCl (~0.18 mol/L), ascorbic acid (20 μL, 100 mg/mL), and HBED-CC-PSMA (compound 1; 10 μg). The crude reaction mixture was loaded onto a SepPak Light C-18 cartridge (Waters Corporation, Milford, Massachusetts) and then washed with water (10 mL) to remove uncomplexed radiometal ions and polar impurities. The radiotracer was eluted in ~0.5 mL 50% EtOH/H_2O, and the product was analyzed by RP-HPLC (Chromolith method: R_t = 2.33 (25%) and 2.38 (75%) min.; specific activity A_s = 42.2 GBq/μmol). Note two species (potentially diastereomers) are formed in an approximate ratio of 1:3. These two species are shown to behave in an identical manner toward PSMA binding in vitro and in vivo.[20] Typical decay-corrected radiochemical yields (RCYs; including both species) were >98% (n = 5) with radiochemical purity (RCP) >98% (n = 5).

*Radiosynthesis of ^{68}Ga-DFO-Nsucc-PSMA (^{68}Ga-**4**).* ^{68}Ga-DFO-Nsucc-PSMA (^{68}Ga-4) was prepared within 10 minutes at room temperature by manual synthesis and using the Modular-Lab PharmTracer module by Eckert & Ziegler (Berlin, Germany). The ^{68}Ga eluate (~600 MBq) was transferred into a reaction vial containing ammonium acetate buffer (2.0 mL, 0.5 mol/L, pH5.2) and DFO-Nsucc-PSMA (compound 4; 10-20 μg). After reaction, the crude mixture was loaded onto a SepPak Light C18 cartridge (Waters Corporation) and washed with water (10 mL) to remove uncomplexed radiometal ions and polar impurities. The radiotracer was eluted in ~0.5 mL 30% EtOH/H_2O, and the product was analyzed by RP-HPLC (Chromolith method: R_t = 2.39 min. (100%); specific activity [A_s] = 27.4 GBq/μmol). Typical decay-corrected RCYs were >98% (n = 8) with RCP >99% (n = 8).

*Radiosynthesis of ^{68}Ga-DFO-pNCS-Bn-PSMA (^{68}Ga-**7**).* ^{68}Ga-DFO-*p*NCS-Bn-PSMA (^{68}Ga-7) was prepared using the same procedure describe for ^{68}Ga-4 (vide supra). The ^{68}Ga-7 radiotracer was eluted from the Sep-Pak Light C18 cartridge in ~0.5 mL 30% EtOH/H_2O, and the product was analyzed by RP-HPLC (Chromolith method: R_t = 2.57-3.13 minutes (100%); A_s = 23.8 GBq/μmol). Typical decay-corrected RCYs were >96% (n = 8) with RCP >98% (n = 8).

Lipophilicity (LogD) measurements

The lipophilicity values of the ^{68}Ga-radiotracers are reported as LogD (*n*-octanol/phosphate-buffered saline [PBS] pH7.4) and were determined using the standard "shake-flask" method.[39,40]

Cells and Tissue Culture

The PSMA-positive LNCaP cells (ATCC, Manassas, Virginia) were cultured at 37°C in a 5% CO_2 atmosphere (RPMI Medium 1640 GlutaMAX containing 1% fetal bovine serum [FBS], 100 U/mL penicillin, 100 μg/mL streptomycin, and sodium–pyruvate 1 mmol/L).

Saturation Binding Experiments In Vitro

For receptor saturation analysis, PSMA(+) LNCaP cells were seeded at a density of 0.8 to 1 million cells per well in 6-well poly-L-lysine (PLL)-coated plates and incubated overnight with medium (RPMI Medium 1640 GlutaMAX containing 1% FBS, 100 U/mL penicillin, 100 µg/mL streptomycin, and 1 mmol/L sodium pyruvate). After 24 hours, the medium was removed, the cells were washed and incubated for 1 hour at 37°C with fresh binding buffer (RPMI Medium 1640 GlutaMAX containing 1% FBS, 100 U/mL penicillin, 100 µg/mL streptomycin, 50 mmol/L HEPES, 50 µg/mL bacitracin, and 0.5% bovine serum albumin). Then the plates were placed on ice for 30 minutes, followed by incubation with increasing concentrations of $^{68/nat}$Ga-radiotracers in PBS-binding buffer (pH7.4) for 120 minutes at 4°C. Nonspecific binding was determined in the presence of excess 2-(phosphonomethyl)pentane-1,5-dioic acid (PMPA; 1 µmol/L). The cells were washed twice with ice-cold PBS and then lysed with 1 mol/L NaOH. The cell-associated radioactivity was measured using a gamma counter. Specific binding was plotted against the total molar concentration of the added radiotracer. The K_d/nM values and the concentration of the radiotracers required to saturate the receptors (B_{max}/nM) were determined by nonlinear regression analysis. In all cellular experiments, the calculated values were normalized to the number of cells per well (typically 1×10^6 cells). Data reported are from 2 independent experiments with triplicate data points in each experiment.

Xenograft Models

All animal experiments were conducted according to the regulations of the University Medical Center of Freiburg, Germany, and in accordance with the principles of the 3Rs and the *Guide for the Care and Use of Laboratory Animals*. Normal athymic Balb/c nude mice (17-20 g, 4-6 weeks old, n = 12) were obtained from Janvier SAS (St Berthevin Cedex, France). Mice were provided with food and water ad libitum. The LNCaP tumors were induced on the right shoulder by subcutaneous (sc) injection of 5.0 million cells in a 100-µL cell suspension of a 1:1 v/v mixture of media with reconstituted basement membrane (GFR BD Matrigel; Corning BV, Amsterdam, Holland). After an average of 4 weeks, the tumor size reached ~200 to 300 mg (estimated by caliper measurements), and the animals were then used for PET imaging studies.

Blood Plasma Protein Binding Studies and Metabolism In Vivo

Mice (n = 2/group) were administered with appropriate formulations of the 3 ^{68}Ga-radiotracers (7.3-11.1 MBq, 0.3-0.4 nmol in 0.2 mL PBS) *via* intravenous tail vein injections. Mice were killed 15 minutes post-radiotracer administration. Blood was collected in heparinized tubes and centrifuged (5 minutes, 1700 g) for plasma isolation. Plasma samples (300 mL) were transferred to an ultrafiltration device (Vivacon 500; 30 kDa molecular weight cutoff [Sartorius Stedium Biotech GmbH, Germany]), and centrifuged (10 minutes, 9660 g) to separate proteins. Samples of the filtrate and protein fraction were measured in the gamma counter. In addition, aliquots of the eluate from ultrafiltration were analyzed by RP-HPLC to assess the extent of radiotracer metabolism in the soluble blood component.

Small-Animal PET Imaging

The PET imaging experiments were conducted on a microPET Focus 120 scanner (Concorde Microsystems, Knoxville, Tennessee).[41] For static scans, mice were administered ^{68}Ga-radiotracer formulations (15.4-18.7 MBq, ~0.56-0.68 nmol in 200 µL sterile filtered PBS pH7.4 [Note: the ethanol content was <8% for all formulations]) via intravenous tail vein injection. For dynamic scans, a higher dose of radioactivity (~28 MBq, ~0.9-1.0 nmol) was administered to ensure adequate counting statistics during reconstruction of comparatively short timing windows (from between 20 seconds and 5 minutes). Approximately 5 minutes prior to recording PET images, mice were anesthetized by inhalation of 2% to 3% isoflurane/oxygen gas mixture, fitted with an intravenous catheter (dynamic scans), and placed on the scanner bed in the prone position. Anesthesia was maintained using 1% to 2% isoflurane. The PET images were recorded at various time points between 0 and 3 hours postinjection. Dynamic scans were recorded for 3500 seconds postradiotracer administration and temperature was maintained using a heating pad. List-mode data were acquired using a γ-ray energy window of 350 to 650 keV and a coincidence timing window of 6 nanoseconds. The PET sinograms were reconstructed using a 2-dimensional ordered subset expectation maximization algorithm. Image counts per second per voxel were calibrated to activity concentrations (Bq/g) by measuring a 3.5-cm cylinder phantom filled with a known concentration of radioactivity and mass. For quantification of tumor radioactivity uptake in the PET scans, small 3-dimensional volumes-of-interest (VOIs) were drawn manually using AMIDE Medical Image Data Examiner software,[42] and the decay corrected mean percentage injected dose per gram (%ID/g) in various tissues was determined.

Competitive inhibition (blocking) studies were also performed in vivo using static PET imaging to investigate the specificity of the ^{68}Ga-radiotracers for PSMA. Nonradiolabeled PMPA (20 nmol/mouse) was coinjected with the ^{68}Ga-radiotracers (n = 3).[43]

Statistical Analyses

Statistical analyses were performed using GraphPad Prism 5.01 (GraphPad Software, Inc, San Diego, California) and Microsoft Excel (Version 15). Data were analyzed using the unpaired, 2-tailed Student *t* test. Differences at the 95% confidence level ($P < .05$) were considered to be statistically significant.

Table 1. Summary of the In Vitro Characterization Data.

Compound	Molecular Formula	MW (calcd) /g/mol[a]	Specific activity / GBq/μmol	LogD (*n*-octanol: PBS pH7.4)	K_d / nmol/L
^{68}Ga-**1**	$C_{44}H_{58}GaN_6O_{17}S_2^-$	1075.2561	42.2	−4.06 ± 0.10	2.89 ± 0.55
^{68}Ga-**4**	$C_{47}H_{79}GaN_{10}O_{18}$	1140.4830	27.4	−3.24 ± 0.05	26.4 ± 7.8
^{68}Ga-**7**	$C_{51}H_{81}GaN_{12}O_{16}S_2$	1250.4591	23.8	−2.60 ± 0.02	13.6 ± 2.6

Abbreviations: ^{68}Ga-1, ^{68}Ga-HBED-CC-PSMA; ^{68}Ga-4, ^{68}Ga-DFO-Nsucc-PSMA; ^{68}Ga-**7**68, Ga-DFO-*p*NCS-Bn-PSMA; PSMA, prostate-specific membrane antigen.
[a]Exact isotopic mass.

Results and Discussion

Synthesis and Radiochemistry

Ligands 4 and 7 were synthesized using standard amide bond or thiourea chemistries in 16% and 76% yield, respectively. A summary of the in vitro characterization data is presented in Table 1. Both compounds gave single peaks in RP-HPLC with >98% chemical purity. The chemical composition of compounds 4 and 7 was confirmed using both low- and high-resolution electrospray ionization mass spectrometry. For compounds 4 and 7, peaks corresponding to the monoprotonated molecular ion $[M+H]^+$ and the diprotonated species $[M+2\ H]^{2+}$ were identified in (+)-LR-ESI-MS. In (+)-HR-ESI-MS only peaks corresponding to the $[M+2\ H]^{2+}$ ions (at *m/z* 538.2981 and 593.2877, for 4 and 7, respectively) were found. Subsequent nonradioactive reactions between ligands 4 and 7 with $Ga(NO_3)_3$ gave the expected peaks at *m/z* 571 and 626 (100%; $[M+2\ H]^{2+}$), respectively. Furthermore, a test reaction between an aqueous solution of ligand 4 and $FeCl_3$ gave an instantaneous color change from colorless to an intense orange/brown, confirming the formation of the Fe-DFO complex. Note that Fe-DFO has a known broad electronic absorption maximum at 430 nm.[16]

Manual and fully automated ^{68}Ga-radiolabeling reactions were optimized in ammonium acetate buffer (0.5 mol/L, pH 5.2, room temperature). ^{68}Ga-radiolabeling of 4 and 7 proceeded quantitatively at room temperature in 10 to 15 minutes. Both radiolabeled compounds ^{68}Ga-4 and ^{68}Ga-7 were isolated from the reaction mixture using a Sep-Pak Light C18 cartridge (Waters Corporation, Milford, MA). After loading the C18 cartridge, the compounds were purified from unreacted $^{68}Ga^{3+}$ ions by washing with water or saline, and the product was eluted with 20% to 30% EtOH/water (v/v). The average RCYs for ^{68}Ga-4 and ^{68}Ga-7 were >98% (n = 8) and >96% (n = 8), with RCP >98%, and specific activities of 27.4 and 23.8 GBq/μmol, respectively. In comparison, using a similar automated synthesis module, ^{68}Ga-1 was isolated with an A_s of 42.2 GBq/μmol. Notably, when higher amounts of initial ^{68}Ga-radioactivity are used in the routine clinical preparation of ^{68}Ga-1, A_ss as high as 75 to 80 GBq/μmol can be achieved. When the initial amount of labeling precursors 4 and 7 was reduced from 20 μg to 10 μg, A_ss of ^{68}Ga-4 and ^{68}Ga-7 increased accordingly and were comparable to that attained for ^{68}Ga-1. Both radiolabeled compounds ^{68}Ga-4 and ^{68}Ga-7 were found to be stable with respect to changes in RCP after incubation in saline or PBS at 37°C for over 4 hours. These data confirmed that no radiolysis or chemical degradation occurred in the formulated samples used for in vitro and in vivo studies.

Lipophilicity measurements for ^{68}Ga-1, ^{68}Ga-4, and ^{68}Ga-7 gave LogD values of −4.06 ± 0.10, −3.24 ± 0.05, and −2.60 ± 0.02, respectively. In comparison to ^{68}Ga-1, the new DFO-conjugated compounds are less hydrophilic. Consistent with the chemical structures of the linker groups, measurements showed that the more hydrophilic succinyl linker/spacer in ^{68}Ga-**4** conveys increased water solubility compared to the aromatic *p*NCS-Bn group in ^{68}Ga-7.

Cellular Assays

Prior to conducting PET imaging in mice, the cellular dissociation constants (K_d/nM) and specificity of $^{68/nat}$Ga-radiotracers 1, 4, and 7 were measured using standard saturation binding experiments in LNCaP PSMA(+) cells (Table 1 and Figure S1).[16,44,45] Across all experiments, estimated receptor concentrations (B_{max} values) were consistent in the range 0.27 to 0.41 nmol/L. Cellular binding data confirmed that both ^{68}Ga-radiotracers of ligands 4 and 7 bind specifically to PSMA expressed on LNCaP cells. The apparent K_d values of ^{68}Ga-4 (26.4 ± 7.8 nmol/L) and ^{68}Ga-7 (13.6 ± 2.6 nM) indicate that these compounds exhibit lower affinity toward PSMA than the current clinical radiotracer ^{68}Ga-7 (2.89 ± 0.55 nmol/L). Typically, a lower binding affinity of a radiotracer would reduce target tissue uptake in PET imaging. However, it is worth noting that specific contrast in PET is influenced by multiple factors including nonspecific uptake, tissue perfusion, cellular internalization, and sequestration which influences retention/washout, metabolic stability, and whole-body excretion. Therefore, PET imaging in tumor-bearing mice was performed to evaluate radiotracer pharmacokinetics.

Positron-Emission Tomography Imaging in Tumor-Bearing Mice

A combination of dynamic (for 3500s) and static PET scans (starting at 30 minutes, 1, 2, and 3 hours postradiotracer administration) were used to assess the pharmacokinetics and specificity of the ^{68}Ga-radiotracers for detecting PSMA expression in mice bearing subcutaneous LNCaP tumors on the right shoulder. Representative static PET images recorded at 1 hour

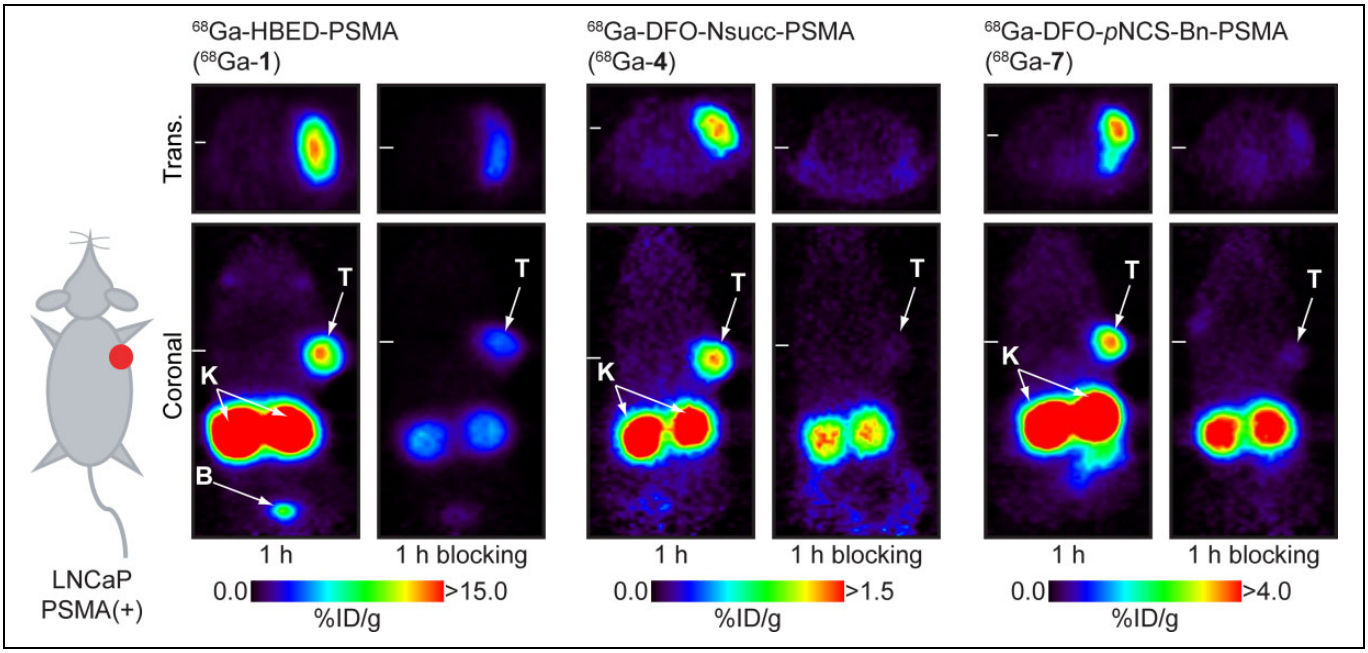

Figure 3. Representative static positron emission tomography (PET) scans of ^{68}Ga-HBED-CC- prostate-specific membrane antigen (PSMA)-(^{68}Ga-**1**), ^{68}Ga- desferrioxamine B (DFO)-Nsucc-PSMA (^{68}Ga-**4**), and ^{68}Ga-DFO-*p*NCS-Bn-PSMA (^{68}Ga-**7**) recorded at 1 hour postradiotracer administration in mice bearing subcutaneous LNCaP tumors (~200-300 mg). In each case, blocking studies confirmed the specificity of the ^{68}Ga-radiotracer for PSMA expression. Note that in the 3 sets of image data, different upper thresholds (in units of %ID/g) have been used for visual clarity in the representation of radiotracer uptake in the tumors. T indicates tumor; K, kidney; B, bladder.

are shown in Figure 3. Additional PET data are presented in Supporting Information Figures S2 to S6. Competitive inhibition studies (blocking using coadministration of PMPA [20 nmol/mouse][43]) confirmed the specificity of the ^{68}Ga-radiotracers for PSMA expression. Time–activity curves (TACs) of the tumor, heart/blood pool, kidney, and bladder measured from VOI analysis of the dynamic PET data are shown in Figure 4.

Imaging data revealed that the 2 radiotracers, ^{68}Ga-4 and ^{68}Ga-7, showed specific accumulation in PSMA(+) LNCaP tumors. In the case of ^{68}Ga-4, peak uptake (~3-4%ID/g) was observed within the first 5 to 10 minutes postadministration, after which, rapid washout of the radioactivity occurred. The tumor washout phase for ^{68}Ga-4 correlated with decreased activity in the heart/blood pool and excretion via the kidneys/bladder (Figure 4). At later time points (1-3 hours), ^{68}Ga-4 tumor uptake/retention showed higher accumulation in tumors than the background due to perfusion (Figures S3 and S4). However, after 3 hours postadministration, absolute tumor uptake of ^{68}Ga-4 remained very low (~0.8-1.2%ID/g).

In dynamic PET, ^{68}Ga-7 showed similar peak tumor uptake (~3.5-4.0%ID/g) to ^{68}Ga-4 but overall had a dramatically different pharmacokinetic profile. Heart/blood pool activity of ^{68}Ga-7 remained higher at each time point in the dynamic scans, and in contrast to the rapid tumor washout observed for ^{68}Ga-4, tumor-associated radioactivity showed slower washout for ^{68}Ga-7 (2.90 $\pm$ 0.46%ID/g after 3500 seconds). Static PET imaging revealed that tumor-associated ^{68}Ga-7 activity was specific and retained at ~2.5-3.5%ID/g for up to 3 hours (Figures S5 and S6 [blocking study]).

Equivalent dynamic and static PET imaging experiments using the standard clinical agent ^{68}Ga-1 showed that this radiotracer has a longer residence time in the heart/blood pool, with considerably higher uptake and retention of radioactivity in both the LNCaP tumors and in the kidneys (Figure 4 and Figure S2). In dynamic scans, ^{68}Ga-1 tumor uptake continued to increase to >8.0%ID/g after 3500 seconds.

Interestingly, the 3 ^{68}Ga-radiotracer studied displayed completely different pharmacokinetic uptake/excretion profiles (see heart/blood pool, kidney and bladder TACs in Figure 4). The TACs showed that each of the ^{68}Ga-radiotracers was extracted from the blood. However, ^{68}Ga-4 was most rapidly cleared from circulation, followed by ^{68}Ga-7 and then ^{68}Ga-1. Clearance is predominantly via a urinary mechanism, and the radiotracers showed specific binding to the kidney (which is known to express PSMA). Kidney TACs confirmed the differences in the behavior of the 3 ^{68}Ga-radiotracers (Figure 4C). Specifically, ^{68}Ga-4 showed a very rapid influx and efflux from the kidney, concordant with low affinity binding to PSMA and a rapid clearance to the bladder. In contrast, ^{68}Ga-7 displayed a broader and more prolonged residence in the kidney tissue with a peak uptake of ~50%ID/g at ~1400 seconds postadministration followed by a slow washout phase. The clinical radiotracer, ^{68}Ga-1, displayed rapid accumulation in the kidney with a maximum around 30%ID/g at ~500 seconds postadministration which was retained for the duration of the dynamic scans.

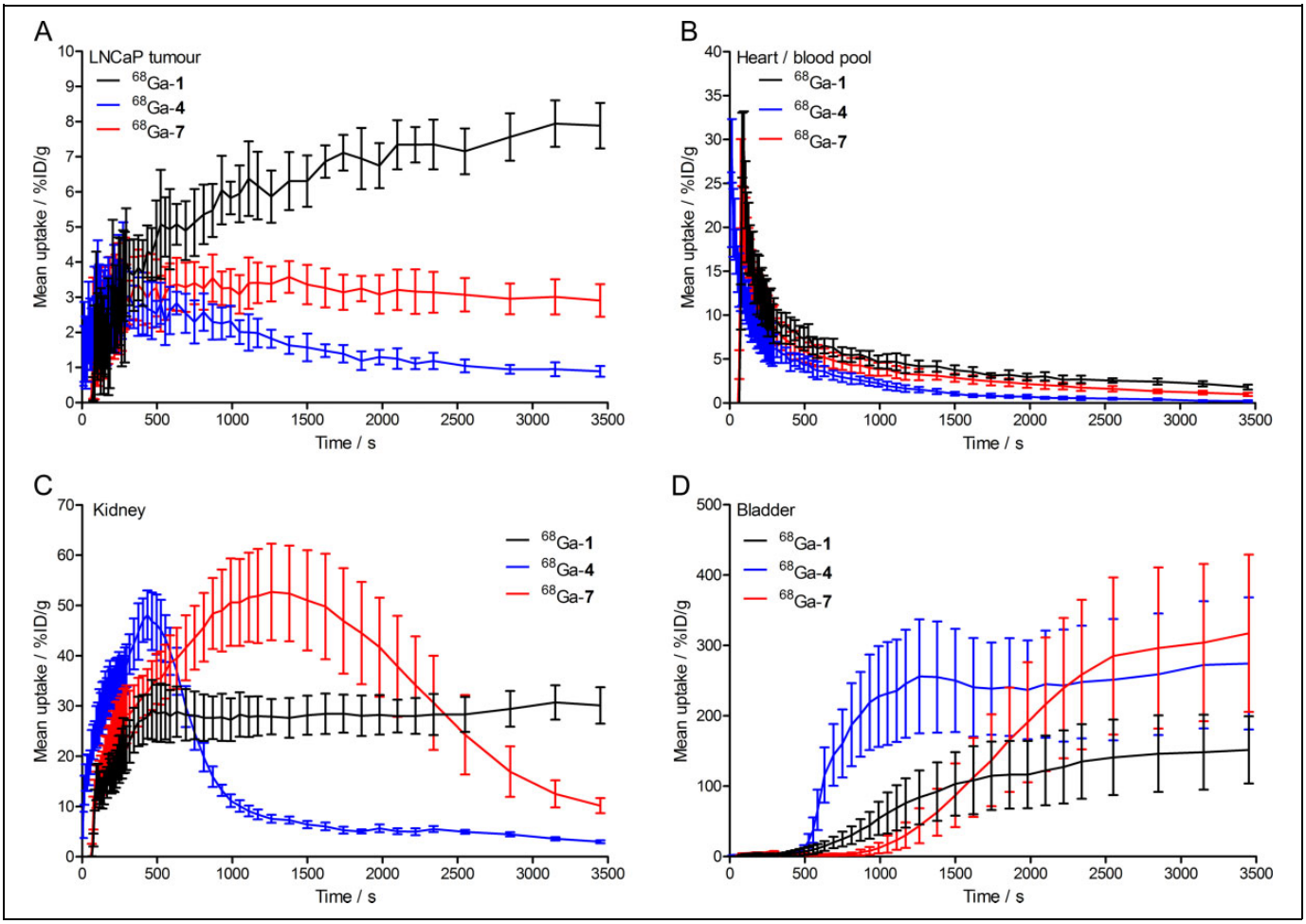

Figure 4. Time–activity curves (TACs) of the accumulation and washout of ^{68}Ga-radioactivity in (A) the tumor, (B) the heart/blood pool, (C) the kidneys, and (D) the bladder from 0 to 30 minutes postadministration of ^{68}Ga-HBED-CC-PSMA (^{68}Ga-1; black), ^{68}Ga-desferrioxamine B (DFO)-Nsucc-PSMA (^{68}Ga-4; blue), and ^{68}Ga-DFO-*p*NCS-Bn-PSMA (^{68}Ga-7; red).

Pharmacokinetic profiles of ^{68}Ga-1 in kidney and bladder are consistent with rapid and specific binding of the radiotracer to the available PSMA. The TAC data suggest that after ~500 seconds postradiotracer administration of ^{68}Ga-1, an equilibrium is reached between uptake and clearance in the kidney. Bladder TACs are consistent with conclusion Figure 4D. The tumor uptake, kidney binding, and bladder excretion profiles of ^{68}Ga-1, ^{68}Ga-4, and ^{68}Ga-7 are consistent with the measured cellular dissociation constants (K_d values; Table 1).

Plasma Protein Binding and Metabolic Stability

To address differences in the pharmacokinetic profiles observed for the 3 ^{68}Ga-radiotracer, ex vivo plasma protein binding and metabolite analyses were conducted using size-exclusion and HPLC methods. Radiotracers were injected into groups of mice and blood samples (n = 2/radiotracer) were taken at 15 minutes postradiotracer administration. Plasma proteins were separated from the soluble component by ultrafiltration and radioactivity counted (Figure 5A). These data revealed that ^{68}Ga-1 had the highest degree of protein association (92% ± 4%), followed by ^{68}Ga-7 (86% ± 2%) and then ^{68}Ga-4 (82% ± 7%). Statistical analysis revealed that protein binding of ^{68}Ga-1 was significantly different (P value <.05) when compared to that of ^{68}Ga-4 and ^{68}Ga-7. Differences between protein binding of ^{68}Ga-4 and ^{68}Ga-7 were not statistically significant (P value >.05). These data are consistent with the heart/blood pool TACs in that increased protein binding correlates with longer blood pool circulation (and consequently, increased delivery and uptake in the LNCaP tumors).

The HPLC analysis of the radioactivity in the soluble fraction of the blood pool revealed that both ^{68}Ga-4 and ^{68}Ga-7 remained 100% intact and chemically unchanged after 15 minutes in mice (Figure 5B). Chemical identity was confirmed by comparison (and spiking) with the isolated ^{68}Ga-4 and ^{68}Ga-7 radiotracers. Similar to reported data for ^{68}Ga-1, these data demonstrated that ^{68}Ga-4 and ^{68}Ga-7 are metabolically stable in mice.[19,20] Therefore, differences in the tumor uptake, PSMA binding, and pharmacokinetics are not associated with radioactive metabolites.

The PET imaging and ex vivo data provide compelling evidence for the stability, sensitivity, and specificity of these urea-

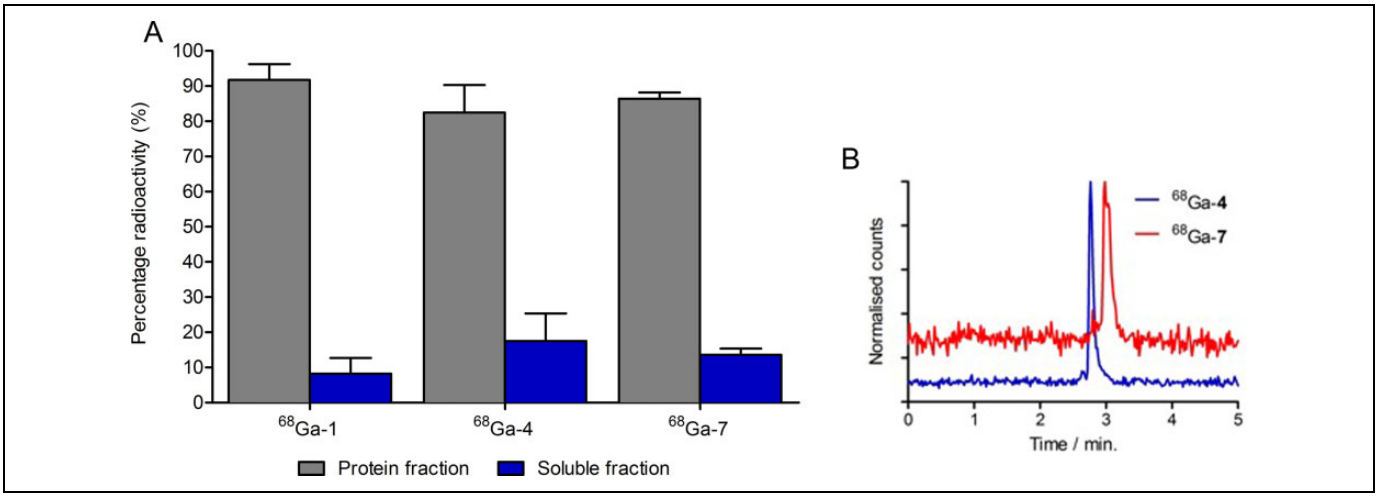

Figure 5. (A) Percentage ^{68}Ga-radioactivity associated with plasma proteins or in solution 15 minutes after injection in mice. (B) High-performance liquid chromatography (HPLC) chromatograms showing the absence of metabolism and single peaks corresponding to ^{68}Ga-desferrioxamine B (DFO)-Nsucc-PSMA (^{68}Ga-4; blue) and ^{68}Ga-DFO-*p*NCS-Bn-PSMA (^{68}Ga-7; red) in the soluble blood component.

based inhibitors for detecting PSMA expression. It is notable that PSMA binding and pharmacokinetics are both highly sensitive toward changes in the structure of the radiotracer (including the chelate, linker, and spacer used to couple the nuclide to the targeting moiety). These data highlight the importance of the chelate and of optimizing all components of a biological targeting construct to achieve the specific contrast.

Conclusion

Two anti-PSMA urea-based radiotracers incorporating DFO as a chelate for coordinating $^{68}Ga^{3+}$ ions have been synthesized, radiolabeled, and evaluated in a series of in vitro and in vivo experiments. Radiolabeling studies found that $^{68}Ga^{3+}$ can be complexed efficiently and rapidly at room temperature using manual or automated methods that yield formulated radiotracers (^{68}Ga-4 and ^{68}Ga-7) in high yields, purity, and specific activity suitable for PET imaging. In contrast to the radiosynthesis of the clinical standard ^{68}Ga-1, the use of DFO as a chelate instead of HBED for ^{68}Ga radiolabeling gives products with a single peak in HPLC. Cellular data (K_d values) showed that ^{68}Ga-4 and ^{68}Ga-7 displayed lower affinity for PSMA expressed on LNCaP cells than ^{68}Ga-1. Dynamic and static PET scans also revealed important differences in the pharmacokinetic profiles of the 3 ^{68}Ga-radiotracers. Each radiotracer showed specific binding and high delineation of PSMA-positive LNCaP tumors. However, in comparison to ^{68}Ga-1, absolute uptake values in the tumor were $\sim$10-fold and $\sim$2.5-fold lower for ^{68}Ga-4 and ^{68}Ga-7, respectively. In addition, blood pool clearance, kidney retention, and urinary excretion profiles were altered dramatically by changing the chelate and linker/spacer groups. Clearance profiles were found to correlate with both plasma protein binding and measured cellular dissociation constants (K_d values) but not with complex lipophilicity (LogD values). Collectively, these data demonstrate that PSMA binding of small-molecule urea-based inhibitors is particularly sensitive to changes in the entire chemical structure from the targeting moiety, through to the spacer group, linker, and chelate (and likely the chemical nature of the radionuclide) employed in radiotracer design.

Acknowledgments

We thank Dr Henrik Braband, Prof Roger Alberto, Michael Benz, and the Mass Spectrometry Service at the University of Zurich for sample analysis.

Declaration of Conflicting Interests

The author(s) declared no potential conflicts of interest with respect to the research, authorship, and/or publication of this article.

Funding

The author(s) disclosed receipt of the following financial support for the research, authorship, and/or publication of this article: Department of Nuclear Medicine, University Hospital Freiburg, the German Cancer Consortium (DKTK), the German Cancer Research Center (DKFZ), the Swiss National Science Foundation (SNSF Professorship PP00P2_163683), and the European Research Council (ERC-StG-2015, NanoSCAN – 676904).

Supplemental Material

Supplementary material for this article is available online.

References

1. Chang SS. Overview of prostate-specific membrane antigen. *Rev Urol*. 2004;6(suppl 10):S13–S18.
2. Wright GL Jr, Grob BM, Haley C, et al. Upregulation of prostate-specific membrane antigen after androgen-deprivation therapy. *Urology*. 1996;48(2):326–334.
3. Gong MC, Chang SS, Watt F, et al. Overview of evolving strategies incorporating prostate-specific membrane antigen as target for therapy. *Mol Urol*. 2000;4(3):217–222;discussion 223.
4. Chen Y, Foss CA, Byun Y, et al. Radiohalogenated prostate-specific membrane antigen (PSMA)-based ureas as imaging

agents for prostate cancer. *J Med Chem*. 2008;51(24): 7933–7943.
5. Srinivasarao M, Galliford CV, Low PS. Principles in the design of ligand-targeted cancer therapeutics and imaging agents. *Nat Rev Drug Discov*. 2015;14(3):203–219.
6. Hillier SM, Maresca KP, Femia FJ, Marquis JC, et al. Preclinical evaluation of novel glutamate-urea-lysine analogues that target prostate-specific membrane antigen as molecular imaging pharmaceuticals for prostate cancer. *Cancer Res*. 2009;69(17): 6932–6940.
7. Vallabhajosula S, Nikolopoulou A, Babich JW, et al. 99mTc-labeled small-molecule inhibitors of prostate-specific membrane antigen: pharmacokinetics and biodistribution studies in healthy subjects and patients with metastatic prostate cancer. *J Nucl Med*. 2014;55(11):1791–1798.
8. Banerjee SR, Pullambhatla M, Byun Y, et al. 68Ga-labeled inhibitors of prostate-specific membrane antigen (PSMA) for imaging prostate cancer. *J Med Chem*. 2010;53:5333–5341.
9. Banerjee SR, Foss CA, Castanares M, et al. Synthesis and evaluation of technetium-99m- and rhenium-labeled inhibitors of the prostate-specific membrane antigen (PSMA). *J Med Chem*. 2008;51(15):4504–4517.
10. Banerjee SR, Foss CA, Pullambhatla M, et al. Preclinical evaluation of 86Y-labeled inhibitors of prostate-specific membrane antigen for dosimetry estimates. *J Nucl Med*. 2015;56(4): 628–634.
11. Alt K, Wiehr S, Ehrlichmann W, et al. High-resolution animal PET imaging of prostate cancer xenografts with three different 64Cu-labeled antibodies against native cell-adherent PSMA. *Prostate*. 2010;70(13):1413–1421.
12. Benešová M, Schäfer M, Bauder-Wüst U, et al. Preclinical evaluation of a tailor-made DOTA-conjugated PSMA inhibitor with optimized linker moiety for imaging and endoradiotherapy of prostate cancer. *J Nucl Med*. 2015;56(6):914–920.
13. Elsasser-Beile U, Wolf P, Gierschner D, Buhler P, Schultze-Seemann W, Wetterauer U. A new generation of monoclonal and recombinant antibodies against cell-adherent prostate specific membrane antigen for diagnostic and therapeutic targeting of prostate cancer. *Prostate*. 2006;66(13):1359–1370.
14. Vallabhajosula S, Kuji I, Hamacher KA, et al. Pharmacokinetics and biodistribution of 111In- and 177Lu-labeled J591 antibody specific for prostate-specific membrane antigen: prediction of 90Y-J591 radiation dosimetry based on 111In or 177Lu? *J Nucl Med*. 2005;46(4):634–641.
15. Milowsky MI, Nanus DM, Kostakoglu L, et al. Vascular targeted therapy with anti-prostate-specific membrane antigen monoclonal antibody J591 in advanced solid tumors. *J Clin Oncol*. 2007; 25(5):540–547.
16. Holland JP, Divilov V, Bander NH, Smith-Jones PM, Larson SM, Lewis JS. 89Zr-DFO-J591 for immunoPET of prostate-specific membrane antigen expression in vivo. *J Nucl Med*. 2010;51(8): 1293–1300.
17. Pandit-Taskar N, O'Donoghue JA, Beylergil V, et al. ^{89}Zr-huJ591 immuno-PET imaging in patients with advanced metastatic prostate cancer. *Eur J Nucl Med Mol Imaging*. 2014;41(11): 2093–2105.
18. Osborne JR, Green DA, Spratt DE, et al. A prospective pilot study of (89)Zr-J591/prostate specific membrane antigen positron emission tomography in men with localized prostate cancer undergoing radical prostatectomy. *J Urol*. 2014;191(5):1439–1445.
19. Eder M, Schäfer M, Bauder-Wüst U, et al. Eisenhut. 68Ga-complex lipophilicity and the targeting property of a urea-based PSMA inhibitor for PET imaging. *Bioconjug Chem*. 2012;23(4): 688–697.
20. Eder M, Neels O, Müller M, et al. Novel Preclinical and radiopharmaceutical aspects of [68Ga]Ga-PSMA-HBED-CC: a new PET tracer for imaging of prostate cancer. *Pharmaceuticals (Basel)*. 2014;7(7):779–796.
21. Afshar-Oromieh A, Avtzi E, Giesel F, et al. The diagnostic value of PET/CT imaging with the (68)Ga-labelled PSMA ligand HBED-CC in the diagnosis of recurrent prostate cancer. *Eur J Nucl Med Mol Imaging*. 2015;42(2):197–209.
22. Afshar-Oromieh A, Malcher A, Eder M, et al. PET imaging with a [68Ga]gallium-labelled PSMA ligand for the diagnosis of prostate cancer: biodistribution in humans and first evaluation of tumour lesions. *Eur J Nucl Med Mol Imaging*. 2013;40(4):486–495.
23. Dietlein M, Kobe C, Kuhnert G, et al. Comparison of [(18)F]DCFPyL and [(68)Ga]Ga-PSMA-HBED-CC for PSMA-PET imaging in patients with relapsed prostate cancer. *Mol Imaging Biol*. 2015;17(4):575–584.
24. Kobe C, Dietlein M, Kuhnert G, et al. The 18F-labeled PSMA_6 compares favorably to 68Ga-labeled PSMA-HBED-CC. A first clinical study in patients with relapsed prostate cancer. *J Nucl Med*. 2015;56:402.
25. Weineisen M, Schottelius M, Simecek J, et al. 68Ga- and 177Lu-labeled PSMA I&T: optimization of a PSMA-targeted theranostic concept and first proof-of-concept human studies. *J Nucl Med*. 2015;56(8):1169–1176.
26. Rahbar K, Ahmadzadehfar H, Kratochwil C, et al. German multicenter study investigating 177Lu-PSMA-617 radioligand therapy in advanced prostate cancer patients. *J Nucl Med*. 2017;58(1): 85–90.
27. Kozikowski AP, Zhang J, Nan F, et al. Synthesis of urea-based inhibitors as active site probes of glutamate carboxypeptidase II: efficacy as analgesic agents. *J Med Chem*. 2004;47(7):1729–1738.
28. Mease RC, Dusich CL, Foss CA, et al. N-[N-[(S)-1,3-dicarboxypropyl]carbamoyl]-4-[18F]fluorobenzyl-L-cysteine, [18F]DCFBC: a new imaging probe for prostate cancer. *Clin Cancer Res*. 2008;14(10):3036–3043.
29. Cho SY, Gage KL, Mease RC, et al. Biodistribution, tumor detection, and radiation dosimetry of 18F-DCFBC, a low-molecular-weight inhibitor of prostate-specific membrane antigen, in patients with metastatic prostate cancer. *J Nucl Med*. 2012; 53(12):1883–1891.
30. Chen Y, Pullambhatla M, Foss C, et al. Synthesis and biological evaluation of [18F]DCFPyL for PSMA-targeted imaging of prostate cancer. *J Nucl Med*. 2011;52:294.
31. Chen Y., Pullambhatla M, Foss CA, et al. 2-(3-{1-Carboxy-5-[(6-[18F]fluoro-pyridine-3-carbonyl)-amino]-pentyl}-ureido)-pentanedioic acid, [18F]DCFPyL, a PSMA-based PET imaging agent for prostate cancer. *Clin Cancer Res*. 2011;17(24):7645–7653. doi: 10.1158/1078-0432.ccr-11-1357.

32. Banerjee SR, Pullambhatla M, Foss CA, et al. ^{64}Cu-labeled inhibitors of prostate-specific membrane antigen for PET imaging of prostate cancer. *J Med Chem*. 2014;57(6):2657–2669.
33. Afshar-Oromieh A, Zechmann C, Malcher A, et al. Comparison of PET imaging with a (68)Ga-labelled PSMA ligand and (18)F-choline-based PET/CT for the diagnosis of recurrent prostate cancer. *Eur J Nucl Med Mol Imaging*. 2014;41(1):11–20.
34. Kularatne SA, Zhou Z, Yang J, Post CB, Low PS. Design, synthesis, and preclinical evaluation of prostate-specific membrane antigen targeted (99m)Tc-radioimaging agents. *Mol Pharm*. 2009;6(3):790–800.
35. Maresca KP, Hillier SM, Femia FJ, et al. A series of halogenated heterodimeric inhibitors of prostate specific membrane antigen (PSMA) as radiolabeled probes for targeting prostate cancer. *J Med Chem*. 2009;52(2):347–357.
36. Cardinale J, Schäfer M, Benešová M, et al. Preclinical evaluation of 18F-PSMA-1007, a new prostate-specific membrane antigen ligand for prostate cancer imaging. *J Nucl Med*. 2017;58(3):425–431.
37. Zanzonico P. Routine quality control of clinical nuclear medicine instrumentation: a brief review. *J Nucl Med*. 2009;49(7):1114–1131.
38. Holland JP, Caldas-Lopes E, Divilov V, et al. Measuring the pharmacodynamic effects of a novel Hsp90 inhibitor on HER2/neu expression in mice using Zr-DFO-trastuzumab. *PloS One*. 2010;5(1):e8859.
39. Wilson AA, Jin L, Garcia A, DaSilva JN, Houle S. An admonition when measuring the lipophilicity of radiotracers using counting techniques. *Appl Radiat Isot*. 2001;54(2):203–208.
40. Waterhouse RN. Determination of lipophilicity and its use as a predictor of blood-brain barrier penetration of molecular imaging agents. *Mol Imaging Biol*. 2003;5(6):376–389.
41. Kim JS, Lee JS, Im KC, et al. Performance measurement of the microPET focus 120 scanner. *Nucl Med*. 2007;48(9):1527–1535.
42. Loening A, Gambhir S. AMIDE: a free software tool for multimodality medical image analysis. *Mol Imaging*. 2003;2(3):131–137.
43. Kratochwil C, Giesel FL, Leotta K, et al. PMPA for nephroprotection in PSMA-targeted radionuclide therapy of prostate cancer. *J Nucl Med*. 2015;56(2):293–298.
44. Troyer JK, Beckett ML, Wright GL Jr. Location of prostate-specific membrane antigen in the LNCaP prostate carcinoma cell line. *Prostate*. 1997;30(4):232–242.
45. Ruggiero A, Holland JP, Hudolin T, et al. Targeting the internal epitope of prostate-specific membrane antigen with 89Zr-7E11 immuno-PET. *J Nucl Med*. 2011;52(10):1608–1615.